nature plants

LETTERS

https://doi.org/10.1038/s41477-018-0117-x

Crosstalk between PTGS and TGS pathways in natural antiviral immunity and disease recovery

Camilla Julie Kørner[1], Nicolas Pitzalis[2], Eduardo José Peña[2,3], Mathieu Erhardt[2], Franck Vazquez[1,4] and Manfred Heinlein[1,2*]

Virus-induced diseases cause severe damage to cultivated plants, resulting in crop losses. Certain plant–virus interactions allow disease recovery at later stages of infection and have the potential to reveal important molecular targets for achieving disease control. Although recovery is known to involve antiviral RNA silencing[1,2], the specific components of the many plant RNA silencing pathways[3] required for recovery are not known. We found that *Arabidopsis thaliana* plants infected with oilseed rape mosaic virus (ORMV) undergo symptom recovery. The recovered leaves contain infectious, replicating virus, but exhibit a loss of viral suppressor of RNA silencing (VSR) protein activity. We demonstrate that recovery depends on the 21–22 nt siRNA-mediated post-transcriptional gene silencing (PTGS) pathway and on components of a transcriptional gene silencing (TGS) pathway that is known to facilitate non-cell-autonomous silencing signalling. Collectively, our observations indicate that recovery reflects the establishment of a tolerant state in infected tissues and occurs following robust delivery of antiviral secondary siRNAs from source to sink tissues, and establishment of a dosage able to block the VSR activity involved in the formation of disease symptoms.

Symptom recovery is characterized by the emergence of asymptomatic leaves following a systemic symptomatic infection. Our observation that *A. thaliana* plants infected with ORMV undergo natural recovery opened the way for a detailed genetic characterization of this phenomenon. Infected plants show a normal development of disease symptoms at 14 days post inoculation (dpi), but from 23–25 dpi all newly emerging leaves show symptom recovery (Fig. 1a and Supplementary Fig. 1). The leaves of plants undergoing recovery show different symptom types from the basal rosette leaves towards the apical leaves (Fig. 1b), that is, non-symptomatic with signs of necrosis (symptom type 1, ST1), symptomatic with different degrees of curling (ST2), symptomatic with strong leaf deformation (ST3) and, finally, symptom-free morphology (ST4). The transition between ST3 and ST4 occurs in 'transition leaves' that show a symptomatic tip and an already symptom-free leaf base (Fig. 1b, arrow). The lack of symptoms in ST4 leaves is not caused by virus exclusion, as these leaves are infected (Fig. 1c) and contain full-length viral genomic as well as the sub-genomic viral plus- and minus-sense RNAs (Fig. 1d). Moreover, infectious virus particles can be isolated from such leaves. Thus, recovery and the suppression of disease symptoms involves the attainment of a virus-tolerant state within these virus-infected tissues.

Because disease symptoms may be caused by the activity of a viral suppressor of RNA silencing (VSR)[4], we monitored VSR activity in plants carrying a double 35S promoter-driven GFP transgene silenced by PTGS (*Arabidopsis* line 8z2[5]). Similarly to several other viruses[6–8], ORMV encodes a strong VSR (the 125k small replicase subunit of the virus) able to revert established silencing. Thus, 8z2 plants did not show symptoms or fluorescence when mock inoculated (Fig. 1e), whereas infection with ORMV led to the recovery of green fluorescence (Fig. 1f), thus revealing the suppression of GFP silencing by VSR activity. Interestingly, green fluorescence was restricted to the symptomatic leaves, while the symptom-free, recovered leaves were non-fluorescent, indicating the lack or strong reduction of VSR activity (Fig. 1f,g). In agreement with the above findings, green fluorescence in the transition leaves (arrow) was present in their symptomatic tips but absent in the recovered leaf base. The separation between the leaf regions with (ST3a) and without (ST3b) green fluorescence occurred along a distinct boundary (Fig. 1h, arrow), suggesting the presence of a physiological switch or threshold above which the VSR no longer provides sufficient activity for effective silencing suppression. Quantitative PCR with reverse transcription (qRT-PCR) experiments confirmed that GFP mRNA levels were high in ST1, ST2 and ST3a but low in ST3b and ST4 (Supplementary Fig. 2a). However, the levels of viral RNA were similar despite the inferred difference in VSR activity between these tissues (Supplementary Fig. 2b, in agreement with Fig. 1d).

The correlation between symptom phenotypes and VSR activity in 8z2 plants was confirmed by specific detection of viral and endogenous sRNAs (Supplementary Fig. 2c). Probing sRNA blots prepared from samples of symptomatic (ST1 and ST2) and non-symptomatic leaves (ST4) revealed the known correlation between tobamoviral VSR activity and specific sRNA accumulation[7,9,10]. As shown previously, miR398* accumulated in ORMV-infected tissue[10]. However, accumulation of this sRNA was restricted to symptomatic tissues with VSR activity (ST1 and ST2) and occurred at much lower levels in recovered tissues lacking strong VSR activity (ST4). Unlike miR398*, miR173 is not influenced by viral infection[10] and showed no specific accumulation patterns as shown previously[10], irrespective whether leaves were symptomatic or recovered. ORMV-derived siRNAs accumulated in symptomatic tissue with high VSR activity (ST1 and ST2) and showed a lower level in recovered tissue. In contrast, GFP-specific siRNAs accumulated in recovered leaves (ST4), which is consistent with the ongoing GFP silencing activity in these tissues.

The correlation between symptom phenotypes and VSR activity was confirmed using the silencing reporter line Suc:Sul[11] expressing an RNA hairpin directed against the SULPHUR gene from the phloem companion cell-specific AtSUC2 promoter. Again, the silencing phenotype was suppressed in symptomatic leaves, whereas

[1]Zurich-Basel Plant Science Center, Department of Environmental Sciences, University of Basel, Basel, Switzerland. [2]Université de Strasbourg, CNRS, IBMP UPR 2357, Strasbourg, France. Present address: [3]Instituto de Biotecnología y Biología Molecular, Facultad de Ciencias Exactas, UNLP-CONICET, La Plata, Buenos Aires, Argentina. [4]MDPI, Basel, Switzerland. *e-mail: manfred.heinlein@ibmp-cnrs.unistra.fr

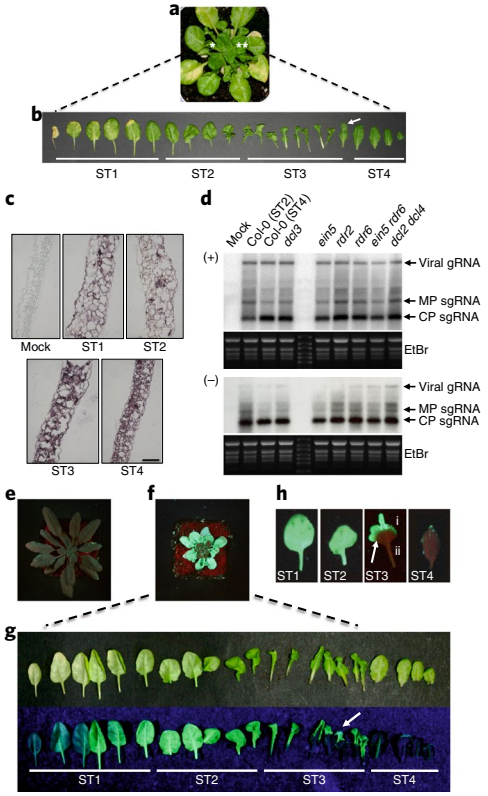

Fig. 1 | Recovered leaves contain virus but have lost strong VSR activity. **a**, ORMV-infected plant at 28 dpi showing symptoms (single asterisk, left) and symptom recovery (two asterisks, right). **b**, Individual leaves of an infected plant at 28 dpi. The leaves show four distinct symptom types: non-symptomatic with signs of necrosis (ST1), curled leaves (ST2), curled leaves with serrated margins (ST3) and non-symptomatic, recovered leaves (ST4). The white arrow indicates the transition leaf between ST3 and ST4 showing symptomatic tip and non-symptomatic base. These symptom recovery phenotypes were seen in twelve recovery experiments, each using at least 4–5 plants. **c**, Demonstration of the presence of genomic viral RNA by in situ hybridization. All symptom types contain high levels of ORMV RNA, as indicated by the coloured signal. Each of the sub-panels is representative of at least 4 individually in situ-labelled sections. The result is confirmed by the northern blot analysis shown in **d**. Scale bar, 100 µm. **d**, Two independent northern blots showing viral plus (+) and minus (−)-sense genomic and sub-genomic viral RNAs in RNA extracts of non-recovered ST2 and recovered ST4 leaves of WT Col-0 plants and in recovered ST4 leaves of different silencing pathway mutants. The viral RNA pattern is identical to the viral RNA patterns reported in previous publications[9,44]. The blot combines independent samples (each sample representing 20 infected plants, that is, recovery experiments) from WT plants (Col-0) and mutants undergoing recovery (*dcl3*, *ein5* and *ein5 rdr6*) or not undergoing recovery (*rdr2*, *rdr6* and *dcl2 dcl4*) in upper leaves, and demonstrates that upper leaves contain full-length plus and minus-sense viral RNA irrespective of recovery. **e**,**f**, *Arabidopsis* PTGS reporter line 8z2 at 28 dpi with mock (**e**) or ORMV (**f**). **g**, Leaves of an ORMV-infected 8z2 plant at 28 dpi, displayed in order with oldest leaves on the left and youngest leaves on the right. The leaves are shown under bright light (top) and UV light (bottom) illumination. The GFP signal seen under UV illumination is indicative of silencing suppression by the virus. The ability of the virus to suppress silencing correlates with symptom types. Recovered leaves are free of observable VSR activity. Transition leaves (arrow) contain VSR activity at the symptomatic tip and no detectable VSR activity at the recovered base. **h**, Expression of GFP indicating VSR activity in leaves of the different symptom types. The transition between silenced (ii) and non-silenced (i) GFP expression in the transition leaf occurs along a sharp border (arrow). Silencing suppression and recovery in this line is easily reproducible and has been observed in three independent experiments.

recovered leaves showed the typical vein-bleaching silencing phenotype (Supplementary Fig. 3).

To further confirm that recovery is due to the loss of VSR activity encoded by the virus, we infected transgenic *Arabidopsis* lines expressing either the p21 VSR of beet yellows virus (BYV)[12] or the p19 VSR of tomato bushy stunt virus (TBSV)[13]. Both lines did not show any symptom recovery following infection. Therefore, we conclude that the loss of efficient VSR activity is a critical determinant in symptom recovery (Supplementary Fig. 4).

Next, we sought to identify RNA silencing pathway components required for symptoms recovery. A collection of *Arabidopsis* mutants impaired in PTGS, miRNA biogenesis, or in RNA decay was infected with ORMV and the development of symptoms was monitored (Table 1, Supplementary Figs. 5-11). *ago1-27* and *hen1-5* mutants impaired in components shared by endogenous siRNA and miRNA pathways, and required for antiviral silencing[14,15], developed symptoms as severe as in WT plants but never developed non-symptomatic, recovered leaves (Supplementary Fig. 5). In contrast, mutants specifically impaired in the biogenesis of miRNAs (*abh1-8*, *cbp20-1*, *se-1*, *dcl1-9*, *hyl1-2* and *hasty* (*hst-15*))[3,16–20] formed normal symptomatic leaves and exhibited normal recovery (Supplementary Fig. 5). The analysis of mutants impaired in the biogenesis of siRNAs (Supplementary Figs. 6 and 7) revealed that most mutants—including *ago7-1*, which is specifically impaired in the biogenesis of TAS3-derived trans-acting siRNAs[3,21,22]—developed symptoms and recovered normally (Supplementary Fig. 6). However, mutants affected in general factors needed for the production and amplification of various siRNA classes (*rdr6-15*, *sgs3-13* and *dcl4-2*)[3] exhibited strong developmental symptoms and did not recover (*rdr6-15* and *sgs3-13*) or recovered only weakly (*dcl4-2*) as compared to the wild type (Supplementary Fig. 7). The ability of the *dcl4-2* mutant to recover from symptoms was probably due to compensation of the lost DCL4 activity by other, partially redundant DCLs, because *dcl2 dcl4* double mutants and *dcl2 dcl3 dcl4* triple mutants did not recover (Table 1, Fig. 2a and Supplementary Fig. 7). These results demonstrate that the symptoms triggered by ORMV are not due to changes in the use or function of miRNAs or ta-siRNAs, and that these sRNA species are not required for recovery. Symptom formation is also independent of accumulated virus-derived siRNAs, since *dcl2 dcl4* double and *dcl2 dcl3 dcl4* triple mutants that are unable to accumulate viral siRNAs[9,23–26] developed symptoms. However, once symptoms are formed, recovery clearly depends on the DCL4/RDR6/SGS3 pathway, which produces primary and secondary endogenous and viral siRNAs[3].

RNA templates required for dsRNA and secondary siRNA synthesis by the DCL4/RDR6/SGS3 pathway are degraded by the 5'–3' exoribonuclease XRN4, which undergoes template competition with RDR6 and acts as an endogenous silencing suppressor by restricting the level of secondary siRNAs[27,28]. Interestingly, XRN4-defective mutants *xrn4-3* and *ein5*[29,30] showed enhanced recovery and recovered earlier than WT plants (Table 1, Fig. 2a,b and Supplementary Fig. 8), thus supporting the importance of RDR6-mediated dsRNA synthesis and secondary siRNA formation in recovery. Because *XRN4* and *EIN5* are allelic and also function in ethylene signalling[29–31], we infected an array of hormonal signalling mutants. However, ethylene as well as salicylic acid (SA), jasmonic acid (JA) and auxin synthesis/signalling mutants developed symptoms and recovered normally (Supplementary Table 1 and Supplementary Fig. 9), showing that enhanced recovery in *xrn4-3* and *ein5* mutants is caused by enhanced silencing and not by a disturbance of ethylene or other hormone signalling in which these genes are involved. The competitive interplay between XRN4 and the DCL4/RDR6/SGS3 pathway was confirmed by the symptom phenotypes of *xrn4-3*, *ein5*, *rdr6-15* single and *ein5 rdr6-15* double mutants (Fig. 2a,b and Supplementary Fig. 8). While *ein5* and *xrn4-3* mutants recovered earlier (before 21 dpi) and developed more recovered leaves than

Table 1 | Occurrence and timing of recovery in PTGS mutants

Timing	ATG number	Mutant	No. of plants[1]	Gene function
Early	AT1G54490	*ein5-1*	14/14	Ethylene signalling/
		xrn4-3	21/22	RNA decay
Normal	AT1G05460	*sde3-4*	4/4	VIGS
	AT2G28380	*drb2*	3/3	dsRNA binding
	AT3G62800	*drb4-1*	3/4	
	AT1G69440	*ago7-1*	4/4	ta-siRNA production
	AT3G05040	*hasty-15*	7/8	miRNA transporter
	AT1G09700	*hyl1-2*	4/4	
	AT1G01040	*dcl1-9*	4/4	miRNA biogenesis
	AT2G27100	*se-1*	4/4	
	AT3G03300	*dcl2-5*	4/4	siRNA biogenesis
	AT1G14790	*rdr1-1*	4/4	
	AT2G13540	*abh1-8/cbp80*	4/4	Cap binding
	AT5G44200	*cbp20*	4/4	
	–	*egs1-1*	4/4	Enhanced silencing
	–	*egs2-2*	4/4	
	AT5G42540	*xrn2-3*	4/4	
	AT1G75660	*xrn3-3*	4/4	Suppressor of PTGS/RNA decay
	AT5G63980	*fry1-6*	4/5	
	AT1G31280	*ago2-1*	4/4	Antiviral defense
	AT1G31290	*ago3-1*	4/4	Unknown
	AT2G27880	*ago5-2*	3/3	Unknown
	AT5G21030	*ago8-1*	4/4	Unknown, pseudogene
	AT5G21150	*ago9-1*	3/3	Ovule development
	AT5G43810	*ago10-1*	3/3	Meristem regulation
Delayed	AT5G20320	*dcl4-2*	7/9	siRNA biogenesis
		dcl3 dcl4	12/12	
	AT3G15390	*sde5-2*	4/4	VIGS
	AT2G15790	*sqn-5*	4/4	Vegetative phase change
None	AT1G48410	*ago1-27*	4/4	PTGS/miRNA
	AT4G20910	*hen1-5*	4/4	
		dcl2 dcl4	4/4	
		dcl2 dcl3 dcl4	4/4	
	AT3G49500	*rdr6-15*	14/14	siRNA biogenesis
		rdr1 rdr6	4/4	
		rdr2 rdr6	4/4	
		rdr1 rdr2 rdr6	4/4	
	AT5G23570	*sgs3-13*	6/6	

[1]The number of plants showing specific recovery phenotype (out of the total number of plants infected). VIGS, virus-induced gene silencing.

the wild type (Fig. 2a,b and Supplementary Fig. 8), *rdr6-15* single mutants did not recover (Fig. 2a and Supplementary Fig. 7), whereas *ein5 rdr6* double mutants recovered like the wild type (Fig. 2b; Supplementary Fig. 8). These results support the hypothesis that *xrn4* mutants recover earlier because of enhanced secondary siRNA production and silencing amplification through RDR6. It is interesting that *ein5 rdr6* double mutants can undergo recovery although *rdr6* single mutants cannot. This could indicate that *rdr6* is partially complemented by another RDR if combined with *ein5*.

Enhanced recovery was also observed in *dcl3-1* (Fig. 2c,d and Supplementary Fig. 8), which is defective in the production of 24 nt siRNAs involved in transcriptional gene silencing (TGS)[3]. Enhanced recovery was maintained in *dcl2 dcl3* double mutants (Table 2; Supplementary Fig. 8) but was lost in *dcl3 dcl4* double mutants (Fig. 2d; Supplementary Fig. 8), indicating that DCL3 antagonizes the antiviral functions of DCL4 and DCL2 during recovery and that this more efficient recovery observed in the absence of DCL3, is DCL4 dependent.

To further investigate a potential role of TGS in recovery, we infected a range of TGS mutants acting up- or downstream of DCL3[3]. As shown in Table 2 (and Supplementary Figs. 8, 10 and 11), none of the mutants, except *dcl3-1*, *dcl2 dcl3* and *drd1-6*, recovered earlier than the wild type, thus further supporting that enhanced recovery in *dcl3-1* occurs through the DCL4-dependent PTGS pathway. Most

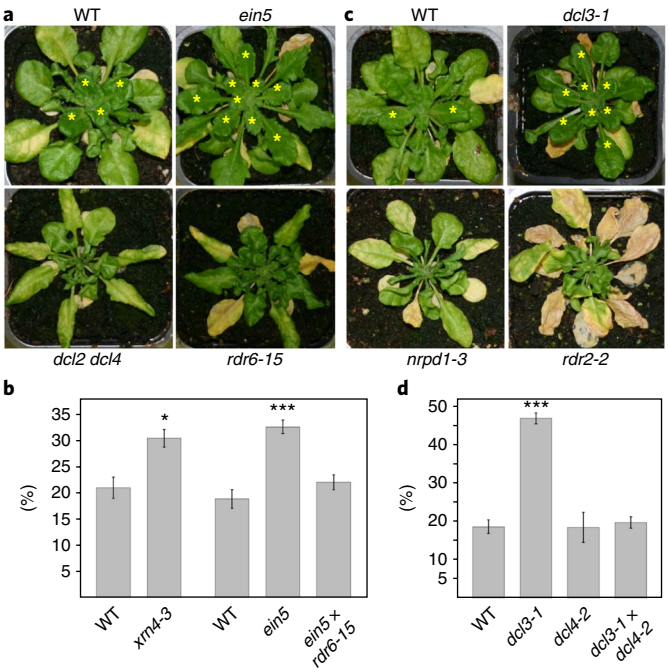

Fig. 2 | The role of PTGS and TGS genes in recovery. a,**b**, *ein5* mutants recover early in an RDR6-dependent manner. **a**, Infected plants at 28 dpi. Yellow asterisks indicate recovered leaves of WT and *ein5* plants. *dcl2 dcl4* and *rdr6-15* mutants did not display any recovered leaves at 28 dpi. **b**, The number of recovered leaves in relation to the total number of leaves at 28 dpi in WT plants, and in *xrn4-3*, *ein5*, and *ein5 rdr6* mutants. $n = 10 \pm$ SE, binomial generalized linear model (GLM), $^{*}P < 0.05$, $^{***}P < 0.001$, compared to respective WT Col-0 plants. The early recovery phenotype of *ein5* plants is RDR6 dependent. **c**,**d**, The role of TGS pathway components in recovery. **c**, Infected plants at 28 dpi. Yellow asterisks indicate recovered leaves. Compared to WT, *dcl3-1* mutants recover early, whereas *nrpd1a-3* and *rdr2-2* mutants failed to recover. **d**, The number of recovered leaves in relation to the total number of leaves at 28 dpi in WT plants as well as in *dcl3-1* and *dcl4-2* single mutants and *dcl3 dcl4* double mutants. $n = 6$–$10 \pm$ SE, binomial GLM, $^{***}P < 0.001$. The early recovery phenotype of *dcl3* mutants is DCL4 dependent.

mutants, including mutants more directly involved in chromatin remodelling and DNA methylation (such as *rdm1*, *drd3*, *classy1*, *drm2*, *dms3*, *rts1*, *ago4* and *ago6*), formed symptoms and recovered normally (Supplementary Fig. 10). However, *rdr2-2* and several Pol IV-subunit mutants —namely *nrpd1a-3*, *nrpd/e2-1* and *drd2-4* (*nrpd/e2*)—did not recover (Table 2, Fig. 2c and Supplementary Fig. 11). These observations demonstrate that recovery depends on the TGS components RDR2 and Pol IV, but that recovery unfolds independently of siRNA-directed DNA methylation.

To further address the mechanism of recovery, we compared the levels of viral RNAs as well as of virus- and host-derived sRNAs between the recovered ST4 leaves of WT Col-0 plants and corresponding upper leaves of *dcl3*, *ein5*, *rdr6* and *rdr2* mutants, and *ein5 rdr6* and *dcl2 dcl4* double mutants. As shown in Fig. 1d, recovered ST4 leaves of WT Col-0 plants contain similar levels of the plus- and minus-sense strands of genomic and sub-genomic viral RNAs as seen in symptomatic ST2 leaves. Moreover, neither the mutations that interfere with recovery (*dcl2 dcl4* and *rdr6*) nor those that enhance recovery (*ein5* and *dcl3*) showed significant effects on viral RNA accumulation in the recovered leaves. This demonstrates that the virus is protected against silencing irrespective of disease symptoms and recovery, and that the formation of symptoms is unrelated to the presence of the virus or its replication. In the respective mutants, the specific RNA silencing pathways and the accumulation of corresponding sRNA species was affected as expected and previously shown[9]. Thus, while none of these mutants affects the formation of miRNAs, the formation of repeat-associated siRNAs and trans-acting siRNAs was inhibited in *dcl3* and *rdr2*, and in *rdr6*, *ein5 rdr6* and *dcl2 dcl4* mutants, respectively (Supplementary Fig. 12). Consistent with the low level of viral siRNAs (vsiRNAs) found in the ST4 leaves of 8z2 plants (Supplementary Fig. 2c), only low vsiRNA levels were present in the recovered ST4 leaves of the WT Col-0 plants. Importantly, ST4 leaves of *dcl3* and *ein5* mutants that showed enhanced recovery contained higher vsiRNA levels, whereas *rdr6* or *dcl2 dcl4* plants, in which recovery is inhibited, contained relatively low or no vsiRNAs, respectively (Supplementary Fig. 12). These observations confirm a role for the DCL2/DCL4/RDR6 pathway in the production of primary and secondary vsiRNAs in recovery.

To determine the nature of reduced or absent VSR activity in recovered leaves, we used a specific antibody to detect the VSR in WT plants and also in mutants in which recovery is either enhanced or inhibited. The results indicate (Supplementary Fig. 13) that recovered leaves contain considerable VSR levels, whereby the VSR levels were lower in *ein5* mutants undergoing early recovery and higher in *rdr6* mutants in which recovery is inhibited. Moreover, as compared to Col-0, VSR levels were higher in 8z2 plants, which contain a constitutive RNA silencing system, and lower in *dcl2 dcl4* plants, in which siRNA synthesis is inhibited. Based on these observations, we conclude that recovery correlates with changes in the expression level as well as with changes in the activity of the VSR.

The analysis of *Arabidopsis* mutants revealed that recovery depends on siRNA biogenesis pathways that produce primary and secondary vsiRNAs. Lack of recovery in *rdr2-2* and in several Pol IV-subunit mutants may indicate a role of RDR2 and Pol IV in viral dsRNA synthesis. However, this explanation appears unlikely given the high levels of vsiRNAs detected in the upper leaves of infected *rdr2* plants (Supplementary Fig. 12). The requirement of RDR2 and Pol IV may suggest that recovery critically relies on mobile vsiRNAs. Indeed, RDR2 and Pol IV are dispensable for the establishment of PTGS but are important for the maintenance and spread of silencing[32–35]. In the current TGS model, RDR2 and Pol IV act in conjunction with DCL3 and AGO4 in the nuclear biogenesis and/or action of siRNAs at methylated genes[36]. However, while DCL3 and AGO4 are required for siRNA-directed DNA methylation, they are dispensable for the cell-to-cell movement of transgene silencing[32,33]. Since our recovery system is also independent of DCL3 and AGO4, as well as of several other tested genes involved in DNA methylation, the genetic requirement for RDR2 and Pol IV in recovery indeed points to a role of intercellular silencing signalling. A role of mobile siRNAs is also suggested by the distinct boundary between recovered and non-recovered tissue in transition leaves. This boundary is reminiscent of the boundary between young and more mature tissues in leaves undergoing the sink-to-source transition, which restricts the movement of viruses, silencing signals and other macromolecules from the sugar-importing sink tissue at the leaf base into the sugar-exporting, already mature, source tissues at the leaf tip[37–39]. Indeed, by infection of plants expressing AtSUC:GFP as a source/sink marker[39] we could demonstrate that recovery occurs in sink leaves and that leaves showing both diseased and recovered areas undergo the sink-to-source transition (Supplementary Fig. 14).

Based on the observed pattern of recovery, the presence of replicating virus and VSR in recovered leaves, and our comprehensive genetic analysis, we propose a model for recovery in which secondary vsiRNAs generated during viral replication move from source to sink leaves. After surpassing a critical threshold, the amount of accumulated vsiRNAs causes oversaturation of local VSR activity and, potentially, translational inhibition of the VSR—the latter

Table 2 | Occurrence and timing of recovery in TGS mutants

Timing	ATG number	Mutant	No. of plants[1]	Gene function
	AT3G43920	*dcl3-1*	13/13	TGS, siRNA biogenesis
Early		*dcl2 dcl3*	4/4	
	AT2G16390	*drd1-6*	13/14	Chromatin remodelling/siRNA-directed DNA methylation
	AT2G40030	*drd3-7 (nrpe1)*	7/7	siRNA-directed DNA methylation; Pol V
	AT3G42670	*classy1-4*	4/4	Spread of RNA silencing
	AT2G36490	*ros1-4*	4/4	DNA de-methylation
	AT5G14620	*drm2-2*	2/2	Methyltransferase, de novo DNA methylation
Normal	AT3G22680	*rdm1-4*	4/4	
	AT3G49250	*dms3-4 (idn1)*	4/4	siRNA-directed DNA methylation
	AT2G27040	*ago4-2*	6/8	
	AT2G32940	*ago6-3*	6/7	siRNA-directed DNA methylation, meristem
	AT5G63110	*rts1-1 (hda6-7)*	6/8	Histone deacetylase
	AT4G11130	*rdr2-2*	4/4	siRNA biogenesis
		rdr1 rdr2	4/4	
None	AT1G63020	*nrpd1a-3*	4/4	
	AT3G23780	*nrpd/e2-1*	4/4	Long-distance PTGS/TGS signalling (Pol IV)
		drd2-4 (nrpd/e2)	4/4	

[1]The number of plants showing specific recovery phenotype (out of the total number of plants infected).

is suggested by reduced 125k VSR accumulation (Supplementary Fig. 13) despite normal levels of viral RNA in ST4 leaves of early recovering mutants (*ein5* and *dcl3*) (Fig. 1d). This model (Fig. 3) is consistent with the observations that mutants accumulating higher levels of secondary vsiRNA (*dcl3-1* and *xrn4*/*ein5)* recover earlier, while mutants impaired in the production of secondary vsiRNA (*dcl2 dcl4, rdr6* and *sgs3*) do not recover. This model is also in agreement with the requirement of RDR2 and Pol IV, indicating the involvement of mobile vsiRNAs. Given our observation that changes in VSR activity or VSR levels allow recovery without causing changes in the accumulation of viral RNA, we propose that the processes leading to disease and disease recovery are determined by VSR activity outside the replication complex. Indeed, although the tobamoviral VSR forms a membrane-bound complex with viral replicase[40], the protein occurs in 10-fold molar excess and its activity is associated with a non-membrane-bound fraction[41]. The tobamovirus VSR suppresses antiviral silencing by siRNA sequestration and interference with their methylation by HEN1[7,42,43]. We propose that the VSR initially interferes with normal plant development and then gets inactivated through saturation by vsiRNAs delivered from source to sink allowing recovery.

The establishment of a recovery system in the model plant *Arabidopsis* allowed us to screen recovery phenotypes in knock-out mutants from various defense pathways. This powerful system led to the identification of individual components or pathways needed for recovery. Based on our results we propose that recovery is initiated in sink tissues and depends on robust secondary 21–22 nt siRNA synthesis and mobility. Moreover, the ability of a plant or its tissues to undergo recovery is under the control of the RNA decay pathways, which compete against the production or stability of 21–22 nt siRNAs available for plant immunity. It has been proposed that recovery may be restricted to viruses with weak VSR activity[1]. However, our observations clearly indicate that recovery can also occur with viruses encoding strong VSRs. Apparently, plants can use RNA silencing coupled to intercellular communication and systemic regulation to gain control over VSR activity in the distant young tissues and thereby overcome an established disease.

Methods

Virus preparation. Virion particles were prepared from ORMV-infected *Nicotiana benthamiana* leaves. Leaves were homogenized to fine powder in liquid N_2. After addition of 1 ml 0.5 M sodium-phosphate buffer (NaP) pH 7.4 and 0.1% 2-mercaptoethanol per g leaf material, virions were extracted with 1 volume butanol/chloroform (1/1 (v/v)) and the phases separated by centrifugation (2 × 15 min at 12,000*g*). Virions in the upper, aqueous phase were precipitated with 4% PEG 8000 at 20,000*g*. The pellet was resuspended in 10 mM NaP pH 7.4 and cleared by centrifugation at 5000*g* for 10 min. The supernatant was precipitated again with 4% PEG 8000 and 1% NaCL and resuspended in 10 mM NaP, pH 7.4. Virion concentration was estimated from absorbance values at 260 nm.

Plant growth conditions, inoculation with virus and screening of mutants. Plants were grown in a Sanyo plant growth chamber (Panasonic, Japan) at 21 °C with 12 h/12 h light/dark cycles. The fifth and sixth leaves of four-week-old plants were each rub-inoculated with 150 ng virions in water or, for mock control inoculations, with water alone. From 18 dpi onwards, plants were monitored for the emergence of recovered leaves. Infected WT Col-0 plants clearly exhibited recovered leaves within 28–32 dpi. Homozygous mutants were screened in comparison to WT Col-0 plants to identify genotypes that are deficient in recovery. The initial screening was performed with 3–4 infected plants and one mock-treated control plant for each genotype. Recovery-deficient genotypes showed a clear-cut phenotype with none of the plants ever undergoing recovery. The 100% recovery-deficient phenotype of these genotypes was reproduced in several subsequent recovery experiments (for example, for isolating material for RNA extraction). For mutants showing recovery, the onset of recovery was usually synchronous within 2–4 days, similarly to the wild type. In case of variation within the genotype, a second experiment was conducted. This particularly applies to genotypes showing changes in the timing of recovery, that is, mutants classified as undergoing enhanced (early) or weak (delayed) recovery. Exact numbers are given in Tables 1 and 2. The recovery phenotype was scored independently by two different individuals. The mutants selected for further investigation based on this screening method all showed clear and reproducible recovery phenotype in all following experiments. Pictures were taken at 28 dpi, unless stated otherwise.

Quantitative RT-PCR. Total RNA was isolated from ground tissue with Trizol reagent (Invitrogen, USA) following the manufacturer's instructions. RNA quantities were determined by spectrophotometric analysis using Nanodrop equipment (Thermo Scientific, USA). 1–2 µg of the RNA preparations were reverse transcribed with random primers using a high-capacity reverse transcriptase (Applied Biosystems, USA). The abundance of specific transcript was measured by probing the cDNA by quantitative PCR using a SYBR-green master mix (Roche, Switzerland) and virus or gene specific primers (Supplementary Table 2) in a Lightcycler 480 (Roche, Switzerland). An internal standard curve using a dilution

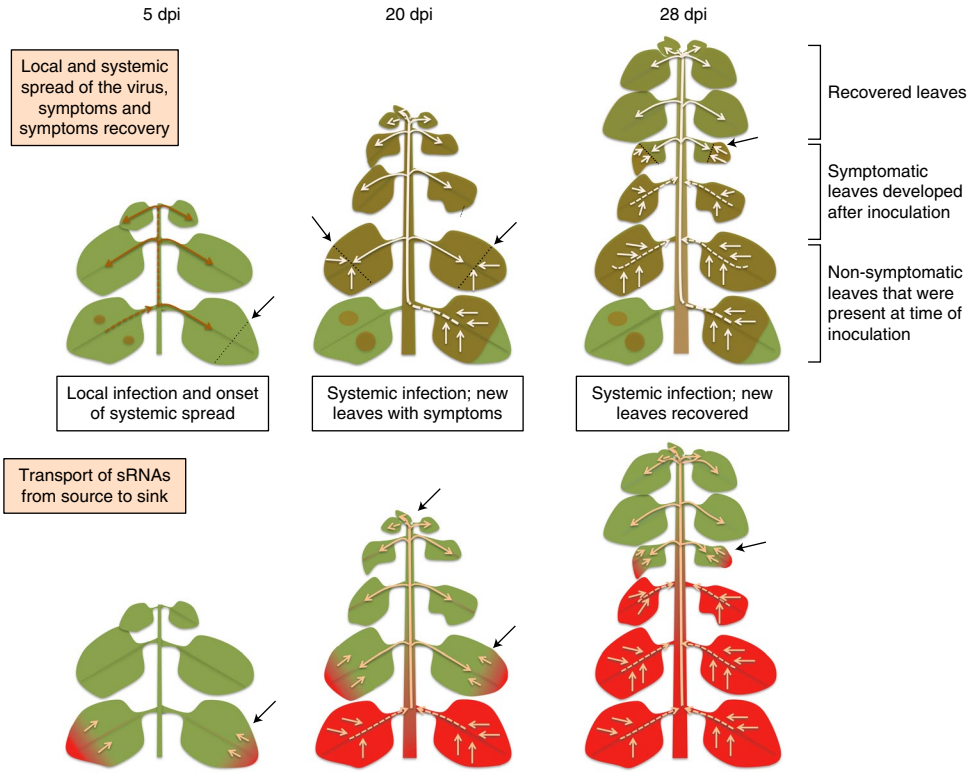

Fig. 3 | Model for recovery. Development of symptoms and subsequent recovery during plant development and the course of infection. At 5 dpi, locally inoculated plants have developed local infection sites (brown spots) from which virus spreads systemically (brown arrows) into sink tissues, including the apical meristem. The virus cannot enter sugar-exporting source parts of the leaves (top: black arrows and dotted line; bottom: sink, green; source, red; light orange arrows, source-to-sink flow). At 20 dpi, the plant is systemically infected (brown, top) and source tissues (red, bottom) export vsiRNAs (white arrows, top) along the source-to-sink flow (light orange arrows, bottom) to sink tissues (green, bottom), including the apical meristem (black arrowhead). Between 5 dpi and 20 dpi, the plant has grown and the sink–source transition now occurs within fully infected leaves (black arrows and dotted lines). The level of mobile vsiRNAs accumulating in sink tissues increases with increasing number of infected and vsiRNA-exporting source leaves. At this stage, the level of vsiRNAs in sink tissues still remains below a critical threshold. All newly developed leaves that emerged since inoculation are infected and show developmental symptoms. At 28 dpi, the amount of infected source tissue has further increased (sink–source transition is indicated by black arrows) and the level of vsiRNAs delivered from source to sink tissues surpassed a critical threshold required for recovery. Local VSR activity is partially saturated and inactivated, allowing normal sRNA-mediated gene regulation to resume. Thus, all recently emerged leaves develop normally and are free of symptoms. Remaining local VSR activity in recovered leaves is sufficient to protect the replicating viral RNA. Mutants in which secondary siRNA synthesis is enhanced (such as the *ein5* and *dcl3* mutants) reach the vsiRNA threshold required for the onset of recovery earlier and, therefore, show enhanced (early) recovery, whereas mutants in which the production or delivery of secondary siRNAs is decreased (such as *dcl4*) or abolished (such as *rdr6*, *rdr2-2* and *nrpd1a-3*) show weak (delayed) or no recovery. Recovery is initiated in sink tissues as soon as the vsiRNA threshold required for recovery is reached, thus explaining the sharp border between recovered and non-recovered tissues seen in transition leaves (ST3a/b). As the plant further develops, the sink-to-source transition, and consequently also the sharp border between diseased source and recovered sink tissues, moves towards younger tissues.

series of pooled cDNA was used for the calculation of relative gene expression. The transcript levels between samples were normalized against the expression of three housekeeping genes (18S, AT1G13440 and AT4G26410).

Northern blotting. Total RNA was extracted from ground tissue using TRI Reagent (Sigma-Aldrich) and fractionated with the RNAeasy Mini Kit (Qiagen), following the RNA cleanup protocol. High- and low-molecular-weight RNA fractions were quantified by spectrophotometric analysis using a Nanodrop device (Thermo Scientific, USA). 8 µg of high-molecular-weight RNA from each sample were separated by formaldehyde agarose electrophoresis and transferred to a nitrocellulose membrane. Viral plus-sense RNA was detected by hybridization with a mix of sense-specific short probes (ORMV_subgen_as_1 to 6; Supplementary Table 2) end-labelled with γ[^{32}P]-dATP. The probes were derived from sequences at the 3' end of the viral RNA genome, thus able to detect full-length viral genomic RNA, as well as the co-terminal sub-genomic RNAs of the virus. Viral negative-sense RNA was detected with a 200 bp long probe synthesized in the presence of α[^{32}P]-UTP by in vitro transcription (RiboMAX; Promega) of a T7 promoter-containing PCR product that was generated from viral cDNA using specific primers (forward: CATCACGAGCTCGAATCAGT; reverse: TAATACGACTCACTATAGGG GGACTTCATGAGAGACTCGT).

sRNAs were detected as previously described[9]. 5 µg total RNA sample (Supplementary Fig. 2c) or 5 µg fractionated low-molecular-weight RNA sample (Supplementary Fig. 12) was separated by electrophoresis through 15 % (Supplementary Fig. 2c) or 16 % (Supplementary Fig. 12) polyacrylamide gels and blotted onto Hybond N + membranes (GE Healthcare, UK). After hybridization with specific probes at 37 °C (Supplementary Fig. 2c) or 40 °C (Supplementary Fig. 12) in Perfect-Hyb buffer (Sigma, USA), blots were washed three times (Supplementary Fig. 12) or five times (Supplementary Fig. 2c) in 2xSSC buffer (300 mM NaCl, 30 mM Na-Citrate, pH 7) containing 0.5% SDS at 37 °C. GFP siRNAs were detected with a GFP-specific PCR fragment (Supplementary Table 2) end-labelled with γ[^{32}P]-dCTP. All other host sRNAs were detected using short probes (Supplementary Table 2) that were end-labelled either with γ[^{32}P]-dCTP (Supplementary Fig S2c) or γ[^{32}P]-dATP (Supplementary Fig. 12). vsiRNAs in Fig S2c were detected with an ORMV-specific radioactively labelled PCR fragment produced by specific forward and reverse primers (Supplementary Table 2). vsiRNAs in Supplementary Fig. 12 were detected with a mixture of three end-labelled oligonucleotide probes (ORMV_1s; ORMV_2s; ORMV_3s; Supplementary Table 2). For detection of different sRNAs in the same RNA extract, blots were stripped by three consecutive washes with boiling 0.5% SDS before re-probing.

In situ hybridization. Leaves were fixed overnight at 4 °C in a FAA solution (formaldehyde 3.2%, acetic acid 5%, ethanol 50%, v/v), dehydrated gradually in 50, 70, 96 and 100% ethanol and infiltrated with paraplast/histoclear (v/v) solution

(VWR International, France). Embedded tissues were sectioned (15 µm) with a Leica microtome. Sections were mounted onto silane (3-aminopropylsilane)-coated microscopic slides, immersed into histoclear solution to remove the paraplast, and rehydrated through 100, 96, 70, 50 and 30% ethanol solutions and distilled water. Before hybridization with specific probes, sections were treated with protease K solution (1 µg ml^{-1}; Sigma, USA) in TE buffer (20 mM Tris-HCl, 5 mM EDTA, pH 7.5) for 15 min at 37 °C, post-fixed with 4% paraformaldehyde, dehydrated through an ethanol series and then air dried for 2 h. A specific RNA probe of 250 nt encompassing part of the coat protein coding region of ORMV was synthesized by in vitro transcription (T7 RNA Pol and ROCHE Dig-RNA labelling mix, Roche, Switzerland) of a T7 promoter-containing PCR product that was generated from viral cDNA using specific primers (forward: CATCACGAGCTCGAATCAGT; reverse: TAATACGACTCACTATAGGG GGACTTCATGAGAGACTCGT). Sections were hybridized overnight at 42 °C with the denatured digoxigenin (DIG)-labelled probe (0.5 µg ml^{-1}) diluted in the hybridization buffer (50% deionized formamide (v/v), 1× Denhardt's solution, 10% dextran sulfate, 4 × SSC, 100 µ g ml^{-1} tRNA, 100 µg ml^{-1} polyA). Tissue sections were washed at 42 °C in 2× SSC, 2× SSC + 0.1% SDS, and 0.2× SSC and then saturated with 0.5% blocking reagent (Roche Diagnostics, Switzerland) diluted in buffer A (100 mM Tris-HCl, 150 mM NaCl, pH 7.5) followed by overnight incubation at 4 °C with anti-DIG-antibodies-AP (dilution 1:1000) (Roche Diagnostics, Switzerland) in buffer A containing 1% BSA (w/v) and 0.1% TritonX-100 (v/v). After washing with buffer A, sections were stained for DIG detection with NBT (nitroblue tetrazolium chloride) and BCIP (5-bromo-4-chloro-3-indolyl-phosphate, 4-toluidine salt) (Roche Diagnostics, Switzerland) in 100 mM Tris-HCl (pH 9.5), 100 mM NaCl, 50 mM $MgCl_2$. Progression of the colour reaction was followed with a microscope and the reaction stopped by washing the section with cold TE buffer (5 min) and water. Slides were mounted in 30% glycerol/TE for microscopy.

Western blotting. Total protein extracts were isolated by grinding plant leaf tissues in liquid N_2 followed by homogenization in extraction buffer (10% glycerol, 5% β-mercaptoethanol, 75 mM Tris-HCl, pH6.8) followed by addition of 2% SDS and heating for 5 min at 95 °C. After centrifugation at 14,000*g* for 10 min and adding 2× Laemmli sample buffer to the aqueous phase, the samples were again heated to 95 °C. Proteins were separated in 10% SDS-PAGE gels, followed by wet blotting to PVDF membranes. The 125k VSR of ORMV was detected with a rabbit antibody raised against a synthetic peptide (GITRADKDNVRTVDS)[44]. As comparison for loading, immunoblots were re-probed with anti-UDP glucose pyrophosphorylase (UGPase) antibodies (Agrisera, Vännäs, Sweden). Signals were detected by luminescence labelling of the primary antibodies with HRP-conjugated secondary antibodies (Pierce, USA).

Life Sciences Reporting Summary. Further information on experimental design is available in the Life Sciences Reporting Summary.

Data availability. The data that support the findings of this study are available from the corresponding author upon request.

Received: 13 November 2015; Accepted: 31 January 2018;
Published online: 1 March 2018

References

1. Ghoshal, B. & Sanfaçon, H. Symptom recovery in virus-infected plants: revisiting the role of RNA silencing mechanisms. *Virology* **479–480**, 167–179 (2015).
2. Ma, X. et al. Different roles for RNA silencing and RNA processing components in virus recovery and virus-induced gene silencing in plants. *J. Exp. Bot.* **66**, 919–932 (2015).
3. Bologna, N. G. & Voinnet, O. The diversity, biogenesis, and activities of endogenous silencing small RNAs in *Arabidopsis*. *Annu Rev. Plant Biol.* **65**, 473–503 (2014).
4. Csorba, T., Kontra, L. & Burgyan, J. Viral silencing suppressors: tools forged to fine-tune host-pathogen coexistence. *Virology* **479–480C**, 85–103 (2015).
5. Glazov, E. et al. A gene encoding an RNase D exonuclease-like protein is required for post-transcriptional silencing in *Arabidopsis*. *Plant J.* **35**, 342–349 (2003).
6. Voinnet, O., Pinto, Y. M. & Baulcombe, D. C. Suppression of gene silencing: a general strategy used by diverse DNA and RNA viruses of plants. *Proc. Natl Acad. Sci. USA* **96**, 14147–14152 (1999).
7. Csorba, T., Bovi, A., Dalmay, T. & Burgyan, J. The p122 subunit of *Tobacco mosaic virus* replicase is a potent silencing suppressor and compromises both small interfering RNA- and microRNA-mediated pathways. *J. Virol.* **81**, 11768–11780 (2007).
8. Dalmay, T., Hamilton, A., Mueller, E. & Baulcombe, D. C. *Potato virus X* amplicons in *Arabidopsis* mediate genetic and epigenetic gene silencing. *Plant Cell* **12**, 369–379 (2000).
9. Blevins, T. et al. Four plant Dicers mediate viral small RNA biogenesis and DNA virus induced silencing. *Nucleic Acids Res.* **34**, 6233–6246 (2006).
10. Hu, Q. et al. Specific impact of tobamovirus infection on the *Arabidopsis* small RNA profile. *PLoS One* **6**, e19549 (2011).
11. Himber, C., Dunoyer, P., Moissiard, G., Ritzenthaler, C. & Voinnet, O. Transitivity-dependent and -independent cell-to-cell movement of RNA silencing. *EMBO J.* **22**, 4523–4533 (2003).
12. Ye, K. & Patel, D. J. RNA silencing suppressor p21 of *Beet yellows virus* forms an RNA binding octameric ring structure. *Structure* **13**, 1375–1384 (2005).
13. Chapman, E. J., Prokhnevsky, A. I., Gopinath, K., Dolja, V. V. & Carrington, J. C. Viral RNA silencing suppressors inhibit the microRNA pathway at an intermediate step. *Genes Dev.* **18**, 1179–1186 (2004).
14. Morel, J. B. et al. Fertile hypomorphic ARGONAUTE (ago1) mutants impaired in post-transcriptional gene silencing and virus resistance. *Plant Cell* **14**, 629–639 (2002).
15. Vaucheret, H. Plant ARGONAUTES. *Trends Plant Sci.* **13**, 350–358 (2008).
16. Kim, S. et al. Two cap-binding proteins CBP20 and CBP80 are involved in processing primary microRNAs. *Plant Cell Physiol.* **49**, 1634–1644 (2008).
17. Vazquez, F., Gasciolli, V., Crété, P. & Vaucheret, H. The nuclear dsRNA binding protein HYL1 is required for microRNA accumulation and plant development, but not posttranscriptional transgene silencing. *Curr. Biol.* **14**, 346–351 (2004).
18. Xie, Z. et al. Expression of *Arabidopsis* miRNA genes. *Plant Physiol.* **138**, 2145–2154 (2005).
19. Lobbes, D., Rallapalli, G., Schmidt, D. D., Martin, C. & Clarke, J. SERRATE: a new player on the plant microRNA scene. *EMBO Rep.* **7**, 1052–1058 (2006).
20. Gregory, B. D. et al. A link between RNA metabolism and silencing affecting *Arabidopsis* development. *Dev. Cell* **14**, 854–866 (2008).
21. Montgomery, T. A. et al. Specificity of ARGONAUTE7-miR390 interaction and dual functionality in TAS3 trans-acting siRNA formation. *Cell* **133**, 128–141 (2008).
22. Jouannet, V. et al. Cytoplasmic *Arabidopsis* AGO7 accumulates in membrane-associated siRNA bodies and is required for ta-siRNA biogenesis. *EMBO J.* **31**, 1704–1713 (2012).
23. Deleris, A. et al. Hierarchical action and inhibition of plant Dicer-like proteins in antiviral defense. *Science* **313**, 68–71 (2006).
24. Donaire, L. et al. Structural and genetic requirements for the biogenesis of *Tobacco rattle virus*-derived small interfering RNAs. *J. Virol.* **82**, 5167–5177 (2008).
25. Bouché, N., Lauressergues, D., Gasciolli, V. & Vaucheret, H. An antagonistic function for *Arabidopsis* DCL2 in development and a new function for DCL4 in generating viral siRNAs. *EMBO J.* **25**, 3347–3356 (2006).
26. Moissiard, G., Parizotto, E. A., Himber, C. & Voinnet, O. Transitivity in *Arabidopsis* can be primed, requires the redundant action of the antiviral Dicer-like 4 and Dicer-like 2, and is compromised by viral-encoded suppressor proteins. *RNA* **13**, 1268–1278 (2007).
27. Gazzani, S., Lawrenson, T., Woodward, C., Headon, D. & Sablowski, R. A link between mRNA turnover and RNA interference in *Arabidopsis*. *Science* **306**, 1046–1048 (2004).
28. Moreno, A. B. et al. Cytoplasmic and nuclear quality control and turnover of single-stranded RNA modulate post-transcriptional gene silencing in plants. *Nucleic Acids Res.* **41**, 4699–4708 (2013).
29. Potuschak, T. et al. The exoribonuclease XRN4 is a component of the ethylene response pathway in *Arabidopsis*. *Plant Cell* **18**, 3047–3057 (2006).
30. Olmedo, G. et al. ETHYLENE-INSENSITIVE5 encodes a 5'→3' exoribonuclease required for regulation of the EIN3-targeting F-box proteins EBF1/2. *Proc. Natl Acad. Sci. USA* **103**, 13286–13293 (2006).
31. De Vleesschauwer, D., Xu, J. & Höfte, M. Making sense of hormone-mediated defense networking: from rice to Arabidopsis. *Front Plant Sci.* **5**, 611 (2014).
32. Smith, L. M. et al. An SNF2 protein associated with nuclear RNA silencing and the spread of a silencing signal between cells in *Arabidopsis*. *Plant Cell* **19**, 1507–1521 (2007).
33. Dunoyer, P., Himber, C., Ruiz-Ferrer, V., Alioua, A. & Voinnet, O. Intra- and intercellular RNA interference in *Arabidopsis thaliana* requires components of the microRNA and heterochromatic silencing pathways. *Nat. Genet.* **39**, 848–856 (2007).
34. Eamens, A., Vaistij, F. E. & Jones, L. NRPD1a and NRPD1b are required to maintain post-transcriptional RNA silencing and RNA-directed DNA methylation in *Arabidopsis*. *Plant J.* **55**, 596–606 (2008).
35. Brosnan, C. A. et al. Nuclear gene silencing directs reception of long-distance mRNA silencing in *Arabidopsis*. *Proc. Natl Acad. Sci. USA* **104**, 14741–14746 (2007).
36. Matzke, M. A. & Mosher, R. A. RNA-directed DNA methylation: an epigenetic pathway of increasing complexity. *Nat. Rev. Genet.* **15**, 394–408 (2014).
37. Roberts, A. G. et al. Phloem unloading in sink leaves of *Nicotiana benthamiana*: comparison of a fluorescent solute with a fluorescent virus. *Plant Cell* **9**, 1381–1396 (1997).
38. Voinnet, O., Vain, P., Angell, S. & Baulcombe, D. C. Systemic spread of sequence-specific transgene RNA degradation in plants is initiated by localized introduction of ectopic promoterless DNA. *Cell* **95**, 177–187 (1998).

39. Imlau, A., Truernit, E. & Sauer, N. Cell-to-cell and long-distance trafficking of green fluorescent protein in the phloem and symplastic unloading of the protein into sink tissues. *Plant Cell* **11**, 309–322 (1999).
40. Watanabe, T. et al. Isolation from *Tobacco mosaic virus*-infected tobacco of a solubilized template-specific RNA-dependent RNA polymerase containing a 126K/183K protein heterodimer. *J. Virol.* **73**, 2633–2640 (1999).
41. Hagiwara-Komoda, Y. et al. Overexpression of a host factor TOM1 inhibits *Tomato mosaic virus* propagation and suppression of RNA silencing. *Virology* **376**, 132–139 (2008).
42. Vogler, H. et al. Modification of small RNAs associated with suppression of RNA silencing by tobamovirus replicase protein. *J. Virol.* **81**, 10379–10388 (2007).
43. Kurihara, Y. et al. Binding of tobamovirus replication protein with small RNA duplexes. *J. Gen. Virol.* **88**, 2347–2352 (2007).
44. Malpica-Lopez, N. et al. Revisiting the roles of tobamovirus replicase complex proteins in viral replication and silencing suppression. *Mol. Plant Microbe Interact.* **31**, 125–144 (2018).

Acknowledgements

This work was supported by funding from the Swiss National Science Foundation (SNF, grant 124940 and 144084 to MH, grant 126329 to FV), the Agence National de la Recherche Scientifique (ANR, grants ANR-08-BLAN-0244 and ANR-13-KBBE-005 to M.H.), the Région Alsace (PhD fellowship to N.P.) and the Centre National de la Recherche Scientifique (CNRS, grant PICS06702 to E.J.P. and M.H.). We would like to thank E. Bucher and T. Blevins for helpful discussions and suggestions, and P. Dunoyer and R. Stadler for providing the SUC:SUL and SUC:GFP *Arabidopsis* lines, respectively. We thank P. Dunoyer for also providing the Col-0 lines expressing the TBSV p19 and the BYV p21 VSRs. We are grateful to M. Pooggin (INRA, Montpellier) for the anti-P125/P182 antibody. Furthermore, we would like to thank M. Böhrer and T. Blevins for their support with RNA blotting and hybridization, and M. DiDonato, A. Niehl, K. Amari and D. Windels for other technical assistance, discussions and critical comments.

Author contributions

F.V. and M.H. conceived and designed the research; C.J.K., N.P., E.J.P., M.E. and M.H. performed the research; C.J.K., N. P., E.J.P., F.V. and M.H. analysed the data; M.E., F.V. and M.H. contributed reagents, materials and analysis tools; C.J.K., F.V. and M.H. wrote the paper; C.J.K, N. P., E.J.P., M.E., F.V. and M.H. read the manuscript and approved the final version of the manuscript.

Competing interests

The authors declare no competing interests.

Additional information

Supplementary information is available for this paper at https://doi.org/10.1038/s41477-018-0117-x.

Reprints and permissions information is available at www.nature.com/reprints.

Correspondence and requests for materials should be addressed to M.H.

Publisher's note: Springer Nature remains neutral with regard to jurisdictional claims in published maps and institutional affiliations.

nature research

Corresponding author(s): Manfred Heinlein

☐ Initial submission ☐ Revised version ☒ Final submission

Life Sciences Reporting Summary

Nature Research wishes to improve the reproducibility of the work that we publish. This form is intended for publication with all accepted life science papers and provides structure for consistency and transparency in reporting. Every life science submission will use this form; some list items might not apply to an individual manuscript, but all fields must be completed for clarity.

For further information on the points included in this form, see Reporting Life Sciences Research. For further information on Nature Research policies, including our data availability policy, see Authors & Referees and the Editorial Policy Checklist.

Experimental design

1. Sample size

Describe how sample size was determined.

The manuscript does not contain statements that require critical quantification (except qRT-PCR experiments. Most experiments rely on phenotyping and direct visual comparison). Sample sizes, where applicable, are provided in the manuscript. Figure 1a,b shows an example of an infected wild type plant showing recovery. Overall, 12 recovery experiments were performed with different sets of homozygous mutants and in all of them the wild type plants (usually a sample size of 4-5 plants) were included as control and showed 100% recovery as shown in Fig. 1a,b and FIg. S1. These experiments included the testing of two different batches of isolated virions used for inoculation (150 ng per leaf, and inoculation of 2 leaves per plant), and the two batches gave the same result. Sample sizes for the testing of mutants for recovery are given in Table 1, Table 2, and Suppl. Table S1. Usually four plants per genotype were tested and more plants were tested when the phenotype was initially unclear. The latter applies in particular to mutants in which the recovery phenotype differed from wild type (mutants showing weak or enhanced recovery). We screened for mutants deficient in recovery. Identified recovery-deficient genotypes showed a clear-cut phenotype with none of the plants undergoing recovery. The 100% recovery-deficient phenotype of these genotypes was reproduced in several subsequent recovery experiments (e.g. for isolating specific leaf material for RNA extraction). Genotypes that maintained the normal ability to recover also showed a clear phenotype with all (or almost all) of the tested plants showing recovery within the expected time period. The phenotype scoring was performed at facilities in Basel using specific conditions in Zanyo-Panasonic growth chambers as specified in Methods. Additional experiments with wt Col-0 as well as several mutants (e.g. ein5, rdr6, rdr2, dc2 dcl4) using large culture chambers in Strasbourg confirmed the results under different growing conditions. All phenotype scoring was performed by at least two of the authors.
Fig. 1 c is based on several in situ hybridization experiments in which we used probes against the positive or negative strand of the virus. The Figure shows representative images from one experiment. Each of the sub-panels is a representative of at least 4 individually in situ-labelled sections. The result is confirmed by the Northern blot analysis shown in Fig. 1d.
Fig. 1d and Fig S12 show long RNA and short RNA Northern blots based on the same plant samples. Sample size was 20 plants for each genotype (each plant in each sample representing an individually scored recovery experiment = 20 replicates per lane). Recovered leaves or the respective, uppermost non-recovered leaves of mutants not able to undergo recovery were pooled before RNA extraction. The sRNA analysis (Fig. S12) of the same plants confirmed the genotypes of the silencing pathway mutants used in the experiment. Loading controls are shown. The sRNA Northern blot has been done once. This is fully sufficient since the pattern of detected viral RNAs is identical to the patterns of viral RNAs in previous publications (Blevins et al. 2006, NAR34, 6233-6246; Malpica-Lopez et al. 2018, MPMI 31, 125-144). Moreover, the presence of full-length viral RNA in recovered and non-recovered leaves is shown in several mutants as well as wild type (each representing an independent sample created from 20 replicates, thus providing mutual confirmation of the answer to the question asked) in the same blot. The presence of full-length viral RNA in

recovered leaves of Col 0 plants was already shown previously on at least one other Northern blot.
Fig. 1 e-g shows recovery in line 8z2 and its correlation with VSR activity. Silencing suppression and recovery in this line is easily reproducible and has been observed in three independent experiments.
Fig 2: Sample sizes for recovery phenotypes are given in Table 1, Table 2, and Table S1. Sample sizes of an independent experiment for the statistics in Fig. 2b,d are given in the legend. The statistical method, standard error and p-values are shown.
Fig. S1: The pattern of plant development and the occurrence of symptom development and recovery shown in this Figure was reproduced several times within the 12 recovery experiments (with usually 4-5 plants per genotype).
Fig S2 a, b: Sample sizes for the qRT-PCR experiments are indicated in the legend. n= 3 means that three different RNA samples (pool of at least 3 plants) for each symptom phenotype were used. Equal amounts of RNA were used for cDNA analysis and the qPCR was standardized to three different reference mRNAs. Each biological sample was run in triplicate (= 3 technical replicates).
Fig S2c: This Northern blot is in agreement with previously reported results, as described in the text. The Fig is also in agreement with Fig S12.
Fig S3 shows recovery in the Suc:Sul line and its correlation with VSR activity. Silencing suppression and recovery in this line is easily reproducible and has been observed in independent experiments.
Fig. S4: Shows suppression of recovery in VSR expressing plants. The experiments have been done twice each with 12 out of 12 infected plants (of each VSR-expressing line) showing suppressed recovery.
Fig S5-S11 show the recovery phenotypes of mutants. Each phenotype is representative of several replicates (see Table 1, Table 2, and Table S1).
Fig. S12 shows a small RNA analysis in the samples also used for long mRNA detection in Fig. 1d. Sample size was 20 plants for each genotype (each plant in each sample representing a scored recovery experiment). Recovered leaves or the respective, uppermost non-recovered leaves of mutants not able to undergo recovery were pooled before RNA extraction.
Fig. S13: The Western blot shows the presence of VSR irrespective of recovery in the upper leaves. The statement that VSR is expressed in recovered leaves is confirmed by different samples (wild type and mutant plants). Sample size was 20 plants (upper recovered / non-recovered leaves) for each genotype.
Fig S14: The correlation of recovery with sink tissues in source-sink marker plants was performed with several plants and each marker plant was in itself sufficient to support the statements made.

2. Data exclusions

Describe any data exclusions.

When plants older than 5 weeks were inoculated with virus, the plants did not show recovery before bolting. These data were excluded. The plant growing conditions are important for recovery and for reproduction of our results. For example, we observed that under LED illumination conditions the day length had to be adjusted to short days to allow recovery before bolting. Our results are based on specific plant growing conditions as stated in the text.

Fig. 1 c is based on several in situ hybridization experiments in which we used probes against the positive or negative strand of the virus. Probes against the negative strand gave only a very weak signal (consistent with the weak negative strand labeling in the Northern blot shown in Figure 1d), and the respective data were excluded.

3. Replication

Describe whether the experimental findings were reliably reproduced.

Details are also given already under “sample size”.
Figure 1a,b shows an example of an infected wild type plant showing recovery. Overall 12 recovery experiments were performed and in all of them the wild type plants (usually a sample size of 4-5 plants) showed recovery as shown in Figure 1a,b.
Fig. 1 c shows representative images from one in situ labelling experiment (panels can be compared). Each of the sub-panels is a representative of at least 4 individually in situ-labelled sections (technical replicates). Several other

experiments were performed showing the presence of signal in infected tissues and absence of signal in mock-treated tissues. The presence of viral RNA in ST4 leaves is confirmed by Northern blotting (Fig 1d).
Fig. 1d and Suppl Fig S12 show long RNA and short RNA Northern blots based on the same plant samples. Sample size was 20 plants for each genotype (each plant in each sample representing a scored recovery experiment). The long mRNA blot shown in the Figure was performed several times to improve quality. The pattern of viral full-length and subgenomic RNAs is known (e.g. Blevins et al., 2006) and reproduced here.
Fig. 1 e-g: Silencing suppression and recovery in the 8z2 line is easily reproducible and has been observed in three independent experiments.
Fig 2: The recovery phenotypes have been seen in several recovery scoring experiments (we preformed 12 experiments with different sets of wild type and mutant Arabidopsis lines) and numbers of plants showing or not showing recovery are summarized in Table 1, Table 2, and Table S1.
Fig. S1: The pattern of plant development and the occurrence of symptom development and recovery in wild type plants was reproduced several times.
Fig S2 a, b: The qRT-PCR experiment combines individual measurements of three biological replicates for each sample. The levels of GFP mRNA are consistent with (and therefore
confirm) the GFP expression pattern in infected L8z2 plants. The variability seen by the standard error bars reflects the variability between the biological replicates.
Fig S2c: This Northern blot was done once. It is reliable as it is in agreement with previously reported results as described in the text.
Fig S3: shows recovery in the Suc:Sul line and its correlation with VSR activity. Silencing suppression and recovery in this line is easily reproducible and has been observed in independent experiments.
Fig. S4: Shows suppression of recovery in VSR expressing plants. The experiments have been done twice. In each experiment, 12 out of 12 infected plants (of each VSR-expressing line) show the suppression of recovery. Thus, this result is easily reproducible.
Fig S5-S11 show the recovery phenotypes of mutants. Each phenotype is only one representative out of several plants (biological replicates) that were individually scored (see Tables 1, 2, S1).
Fig. S12: the sRNA Northern blot was done once and shows the expected sRNA accumulation pattern for the wild type and mutants. Although confirmatory, this sRNA analysis blot was requested by the reviewers.
Fig. S13: The Western blot is a representative of four Western blot experiments supporting the same statement (presence of VSR irrespective of recovery in the upper leaves).
Fig S14: The correlation of recovery with sink tissues in source-sink marker plants was performed with several plants and each marker plant was in itself sufficient to support the statements made.

4. Randomization

Describe how samples/organisms/participants were allocated into experimental groups.

We did not apply randomization. We used specific mutants and analyzed effects of of underlying mutations on recovery.

5. Blinding

Describe whether the investigators were blinded to group allocation during data collection and/or analysis.

We did not apply any blinding in phenotyping the mutants (each plant was labeled with its genotype, and we scored about 70 different genotypes). However, phenotyping was mutually confirmed by the authors.

Note: all studies involving animals and/or human research participants must disclose whether blinding and randomization were used.

6. Statistical parameters

For all figures and tables that use statistical methods, confirm that the following items are present in relevant figure legends (or in the Methods section if additional space is needed).

n/a	Confirmed
☐	☒ The exact sample size (*n*) for each experimental group/condition, given as a discrete number and unit of measurement (animals, litters, cultures, etc.)
☐	☒ A description of how samples were collected, noting whether measurements were taken from distinct samples or whether the same sample was measured repeatedly
☐	☒ A statement indicating how many times each experiment was replicated
☐	☒ The statistical test(s) used and whether they are one- or two-sided (note: only common tests should be described solely by name; more complex techniques should be described in the Methods section)
☒	☐ A description of any assumptions or corrections, such as an adjustment for multiple comparisons
☐	☒ The test results (e.g. *P* values) given as exact values whenever possible and with confidence intervals noted
☐	☒ A clear description of statistics including central tendency (e.g. median, mean) and variation (e.g. standard deviation, interquartile range)
☐	☒ Clearly defined error bars

See the web collection on statistics for biologists for further resources and guidance.

Software

Policy information about availability of computer code

7. Software

Describe the software used to analyze the data in this study.	We used commonly available software (Excel and light cycler 480 (Roche) software) for qRT-PCR analysis. R was used for binomial GLM and bar graphs. Powerpoint and Photoshop were used for Figure assembly (only adjusting brightness-contrast in some cases). Northern and Western blots were created as shown.

For manuscripts utilizing custom algorithms or software that are central to the paper but not yet described in the published literature, software must be made available to editors and reviewers upon request. We strongly encourage code deposition in a community repository (e.g. GitHub). *Nature Methods* guidance for providing algorithms and software for publication provides further information on this topic.

Materials and reagents

Policy information about availability of materials

8. Materials availability

Indicate whether there are restrictions on availability of unique materials or if these materials are only available for distribution by a for-profit company.	All unique materials are available from the authors. Third-party material (as indicated in the Acknowledgements) should be requested from these third parties.

9. Antibodies

Describe the antibodies used and how they were validated for use in the system under study (i.e. assay and species).	anti-P125/P182 antibody was used in Western blot analysis as previously published (Malpica-Lopez et al., 2017). Appropriate controls were used in the experiments to control for sample loading and antibody specificity.

10. Eukaryotic cell lines

a. State the source of each eukaryotic cell line used.	No eukaryotic cell lines were used.
b. Describe the method of cell line authentication used.	No eukaryotic cell lines were used.
c. Report whether the cell lines were tested for mycoplasma contamination.	No eukaryotic cell lines were used.
d. If any of the cell lines used are listed in the database of commonly misidentified cell lines maintained by ICLAC, provide a scientific rationale for their use.	No commonly misidentified cell lines were used.

Animals and human research participants

Policy information about studies involving animals; when reporting animal research, follow the ARRIVE guidelines

11. Description of research animals

Provide details on animals and/or animal-derived materials used in the study.	No animals were used.

Policy information about studies involving human research participants

12. Description of human research participants

Describe the covariate-relevant population characteristics of the human research participants.	This study did not involve human research participants.